RESEARCH ARTICLE

Intracytoplasmic Copper Homeostasis Controls Cytochrome *c* Oxidase Production

Seda Ekici,[a]* Serdar Turkarslan,[b] Grzegorz Pawlik,[c] Andrew Dancis,[d] Nitin S. Baliga,[b] Hans-Georg Koch,[c] Fevzi Daldal[a]

Department of Biology, University of Pennsylvania, Philadelphia, Pennsylvania, USA[a]; Institute for Systems Biology, Seattle, Washington, USA[b]; Institut fur Biochemie und Molekularbiologie, ZBMZ, Albert-Ludwigs-Universität Freiburg, Freiburg, Germany[c]; Department of Medicine, Division of Hematology-Oncology, University of Pennsylvania, Philadelphia, Pennsylvania, USA[d]

* Present address: Seda Ekici, Department of Microbiology, University of Washington, Seattle, Washington, USA.

ABSTRACT **Copper is an essential micronutrient used as a metal cofactor by a variety of enzymes, including cytochrome *c* oxidase (Cox). In all organisms from bacteria to humans, cellular availability and insertion of copper into target proteins are tightly controlled due to its toxicity. The major subunit of Cox contains a copper atom that is required for its catalytic activity. Previously, we identified CcoA (a member of major facilitator superfamily transporters) as a component required for cbb_3-type Cox production in the Gram-negative, facultative phototroph *Rhodobacter capsulatus*. Here, first we demonstrate that CcoA is a cytoplasmic copper importer. Second, we show that bypass suppressors of a *ccoA* deletion mutant suppress cbb_3-Cox deficiency by increasing cellular copper content and sensitivity. Third, we establish that these suppressors are single-base-pair insertion/deletions located in *copA*, encoding the major P1B-type ATP-dependent copper exporter (CopA) responsible for copper detoxification. A *copA* deletion alone has no effect on cbb_3-Cox biogenesis in an otherwise wild-type background, even though it rescues the cbb_3-Cox defect in the absence of CcoA and renders cells sensitive to copper. We conclude that a hitherto unknown functional interplay between the copper importer CcoA and the copper exporter CopA controls intracellular copper homeostasis required for cbb_3-Cox production in bacteria like *R. capsulatus*.**

IMPORTANCE **Copper (Cu) is an essential micronutrient required for many processes in the cell. It is found as a cofactor for heme-copper containing cytochrome *c* oxidase enzymes at the terminus of the respiratory chains of aerobic organisms by catalyzing reduction of dioxygen (O_2) to water. Defects in the biogenesis and copper insertion into cytochrome *c* oxidases lead to mitochondrial diseases in humans. This work shows that a previously identified Cu transporter (CcoA) is a Cu importer and illustrates the link between two Cu transporters, the importer CcoA and the exporter CopA, required for Cu homeostasis and Cu trafficking to cytochrome *c* oxidase in the cell.**

Received 5 December 2013 **Accepted** 9 December 2013 **Published** 14 January 2014

Citation Ekici S, Turkarslan S, Pawlik G, Dancis A, Baliga NS, Koch H-G, Daldal F. 2014. Intracytoplasmic copper homeostasis controls cytochrome *c* oxidase production. mBio 5(1):e01055-13. doi:10.1128/mBio.01055-13.

Editor Howard Shuman, University of Chicago

Address correspondence to Fevzi Daldal, fdaldal@sas.upenn.edu.

Copper (Cu) is an essential transition metal required as a cofactor for many enzymes involved in various biological processes, including cellular energy production, protection against oxidative damage, iron acquisition, and nutritional immunity for restricting pathogen invasion (1, 2). The redox properties of Cu make it a suitable cofactor to carry out electron transfer reactions. However, these properties also render Cu toxic when present in excess amounts, as it can generate reactive oxygen species (e.g., $^{\cdot}OH$ radicals) that damage cellular components (1, 3). It is thought that no free Cu is available in cells (4). Elaborate pathways with high-affinity and low-affinity transporters, metallochaperones, and specific assembly factors and transcriptional regulators handle Cu from its arrival into the cytoplasm to its insertion into cuproproteins (5).

In eukaryotes, the Ctr-type transporters are known to import Cu into the cytoplasm, and the P1B-type Cu-ATPases are important integral membrane proteins that hydrolyze ATP to extrude Cu out of the cytoplasm to maintain homeostasis. The Ctr-type Cu importers are found exclusively in eukaryotes but not in bacteria, whereas the P1B-type Cu-ATPases are major Cu exporters to control its toxicity in a wide range of organisms (6). In humans, defective P1B-type Cu-ATPases ATP7A and ATP7B lead to Menkes and Wilson's diseases (7) and are associated with Alzheimer's disease and resistance to chemotherapy (8, 9). Bacteria contain at least two kinds of P1B-type Cu-ATPases with different physiological roles in exporting Cu out of the cytoplasm (10, 11). Of these exporters, *Pseudomonas aeruginosa* CopA1 (CopA in *Rhodobacter capsulatus*) has a fast Cu efflux rate and is involved in Cu detoxification, whereas CopA2 (CcoI in *R. capsulatus* [12]) has a slow Cu efflux rate and is required for bacterial cytochrome *c* oxidase (Cox) biogenesis (10). *R. capsulatus* mutants lacking CcoI are unable to produce active Cox and are neither sensitive to, nor phenotypically corrected by, exogenous Cu^{2+} addition (12).

The enzymatic activity of Cox relies on its Cu cofactors (13,

14). Cox has a universally conserved binuclear center composed of Cu and iron of heme (heme-Cu center Cu_B) in subunit I. In addition, there are at least 2 or 3 additional subunits in bacterial aa_3-type Cox and up to 13 subunits in mitochondrial aa_3-type Cox (13). Subunit II of the aa_3-type Cox harbors an additional binuclear Cu center (Cu_A) that acts as the primary electron acceptor. The facultative phototrophic Gram-negative bacterium *Rhodobacter capsulatus* contains a single Cox of the cbb_3-Cox type and has only the Cu_B (and no Cu_A) center (15). cbb_3-Cox is composed of at least four subunits, encoded by the *ccoNOQP* operon. Of these subunits, CcoN contains the Cu_B center that is common to all heme-Cu oxidases (4, 13, 14).

Recently, we identified a novel gene (*ccoA*), which encodes a major facilitator superfamily (MFS) type transporter, and showed that its product (CcoA) is required for cbb_3-Cox production in *R. capsulatus* (16). Mutants lacking CcoA contain less Cu than a wild-type strain and produce very small amounts of cbb_3-Cox, unless supplemented with exogenous Cu^{2+} (~5 μM) (16). In this study, we show that the Cu uptake ability of a strain lacking CcoA is much lower than its isogenic wild-type parent and that a *ccoA* deletion mutant frequently acquires suppressor mutations that bypass the need for CcoA in cbb_3-Cox production. These suppressor strains contain large amounts of cellular Cu and are hypersensitive to exogenous Cu^{2+} (Cu^s). Their molecular analyses by using the next-generation sequencing (NGS) and genome-wide comparisons with wild-type and Δ*ccoA* strains identified single-base-pair insertion/deletion (indel) mutations in *copA*, which encodes the *R. capsulatus* P1B-type Cu-ATPase CopA (homologue of *P. aeruginosa* CopA1 [10]). These frameshift mutations occur at a hot spot formed of 10 consecutive cytosine base pairs and inactivate CopA. Construction of a genomic *copA* deletion mutation in the wild type and in Δ*ccoA* backgrounds demonstrated that both the Cu^s phenotype and restoration of Cox production in the absence of CcoA are due to the inactivation of CopA. The Cu^s phenotype and increased cellular Cu amounts in the absence of CopA fully support a role of CopA in copper export (10). Restoration of the cbb_3-Cox deficiency due to the absence of CcoA by the inactivation of CopA reveals a hitherto unknown link between two copper transport systems in bacteria. CcoA imports the required Cu, and CopA exports excess Cu via a cytoplasmic intermediate(s) to maintain cellular homeostasis and safe delivery of Cu to target cuproproteins such as Cox.

RESULTS

CcoA is a cytoplasmic Cu importer. Previously we showed that a mutant lacking CcoA (Δ*ccoA* mutant [strain SE8]) contained less cellular Cu than a wild-type strain and had almost no cbb_3-Cox unless the growth medium was supplemented with micromolar amounts of Cu^{2+}, pointing to a defect in Cu acquisition (16). Considering that CcoA is homologous to MFS-type transporters (16), which are well-established integral cytoplasmic membrane proteins, kinetics of radioactive ^{64}Cu uptake by whole cells of a mutant lacking CcoA and its isogenic parental strain (MT1131) were examined (Fig. 1). Wild-type (MT1131) cells showed vigorous ^{64}Cu uptake in a time-dependent manner at 35°C but not at 0°C, indicative of catalyzed ^{64}Cu uptake. In contrast, under the same assay conditions, the Δ*ccoA* mutant showed greatly reduced ^{64}Cu uptake rates at both 35°C and 0°C. These data, together with our recent finding that *R. capsulatus* CcoA can complement the Cu import defect of a *Schizosaccharomyces pombe* Ctr-less mutant

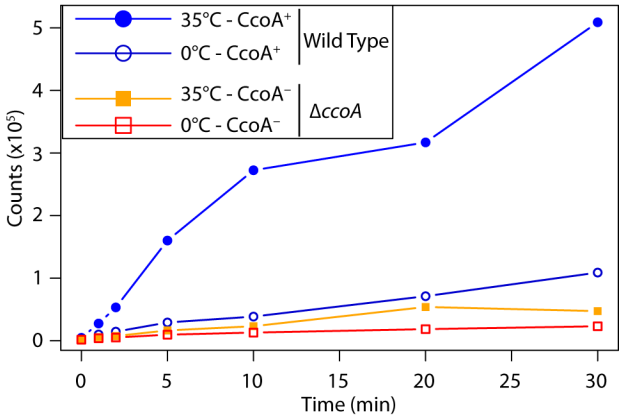

FIG 1 CcoA is required for ^{64}Cu uptake in *R. capsulatus*. Radioactive ^{64}Cu uptake assay by *R. capsulatus* cells was done as described in Materials and Methods. The cells were incubated for 10 min at 0°C or 35°C, ^{64}Cu was added at time zero, and aliquots were taken at 0, 1, 2, 5, 10, 20, and 30 min, and accumulated cellular radioactivity (cpm/7 × 10^7 cells) was determined. Each assay was carried out at least three times using independently grown cells, and typical results are shown.

(17) establish that CcoA is a cytoplasmic Cu importer. Absence of CcoA abolishes Cu import required for normal cbb_3-Cox production in *R. capsulatus*.

Δ*ccoA* revertants are indel mutations in *copA*. We observed earlier that Δ*ccoA* mutants reverted frequently (~10^{-4}) to regain the ability to produce cbb_3-Cox activity (i.e., the $Cox^+/NADI^+$ phenotype) in the absence of Cu^{2+} supplementation (16) (Fig. 2A, left). These Δ*ccoA*Rev revertants (SE8Ri, i = 1, 2, 3. . .) also became Cu^s and accumulated larger amounts of cellular Cu than a Δ*ccoA* mutant or a wild-type strain in the presence and absence of Cu^{2+} supplementation (16) (Fig. 2B, right). Furthermore, upon growth in the presence of 5 μM Cu^{2+}, their colony morphology on solid medium changed from typical *R. capsulatus* smooth (shiny/mucoid) to rough (dry/textured) colonies. In liquid medium, these cultures displayed a reddish color (unlike the usual green color of our laboratory wild-type *R. capsulatus*). Importantly, in these strains, the gain of $Cox^+/NADI^+$ and Cu^s phenotypes as well as increased cellular Cu contents occurred concomitantly, suggesting that the reversion mutation(s) affected cellular Cu homeostasis (16).

In order to uncover the molecular mechanism underlying the restoration of Cox^+ activity in the *ccoA* revertants, we used next-generation sequencing (NGS) for a whole-genome comparison approach. As our *ccoA* mutant and its revertants were derived from our laboratory strain MT1131, the whole-genome sequence of MT1131 together with a *ccoA* mutant and four independent *ccoA* revertants (SE8R1, -2, -5, and -6) were determined and pairwise compared. High genome-wide coverage of analyzed samples (12 to 15 million 100-bp paired-end reads with ~300× coverage) allowed identification of candidate genes that differed from each other by a single nucleotide polymorphism (SNP). Inclusion of two independent cultures of Δ*ccoA* (strain SE8) and Δ*ccoA*Rev1 (strain SE8R1) also monitored possible genome changes that could arise during strain construction and propagation. Strain MT1131 is thought to be derived from strain SB1003 (18) and carries a mutation inactivating the carotenoid biosynthesis gene *crtD*. Whole-genome sequence comparisons between strain

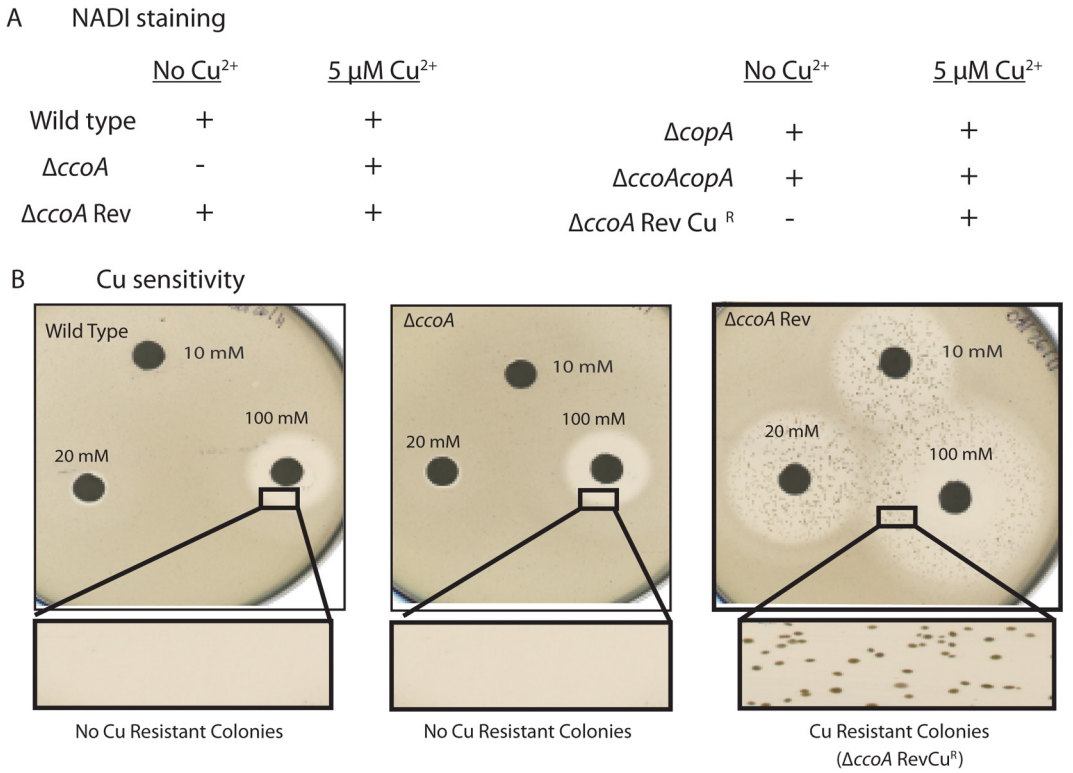

FIG 2 NADI/Cox and Cu^{2+} resistance or sensitivity phenotypes of *R. capsulatus* mutants. (A) NADI staining. Wild type (MT1131), Δ*ccoA* (SE8), Δ*ccoA*Rev (SE8R1or SE8R2), Δ*copA* (SE24), Δ*ccoA* Δ*copA* (SE25), Δ*ccoA*RevCu^R (SE8R1Cu^R or SE8R2Cu^R) strains were grown under aerobic respiratory conditions at 35°C on enriched MPYE medium (44) alone or supplemented with 5 μM $CuSO_4$. NADI/Cox-positive (i.e., colonies turn blue immediately [<0.5 min] when exposed to NADI stain) and NADI/Cox-negative (i.e., colonies do not turn blue over a long period of time [over 10 min]) phenotypes are indicated with + and −, respectively. (B) Cu sensitivity. Cu^{2+} response phenotypes of wild-type *R. capsulatus* (MT1131), Δ*ccoA* mutant (SE8), and its revertant Δ*ccoA*Rev (SE8R1 or SE8R2) were determined by plate growth assays using filter paper disks (soaked in 10 mM, 20 mM, or 100 mM of Cu^{2+} solutions) placed on top of solidified top agar containing the appropriate strains.

MT1131 and the previously sequenced SB1003 strain (19) indeed defined the *crtD121* mutation (C-to-T change at position 753,947 in *crtD121* [RCC00683]) in *R. capsulatus* MT1131 and also revealed the presence of ~1,260-bp deletion (from positions 3,211,370 to 3,212,630) next to a transposase gene, as well as ~385 SNPs and indels across the whole genome (see Table S3 in the supplemental material and http://networks.systemsbiology.net/rcaps/). As expected, the genetically constructed deletion-insertion (starting at position 2,366,510) to knock out *ccoA* was present in SE8 and SE8Ri genomes. Pairwise comparison of the SNPs between all strains showed only one difference for SE8R2 (in the intergenic region upstream of RCC02563-hypothetical protein), SE8R5 (in RCC01565) and SE8R6 (in RCC01100) (Table S3). However, when the indels were compared, a single difference in the RCC01180 gene (at position 1,253,275) annotated as "*copA*, copper translocating P-type ATPase" was found between the wild type (MT1131) and the Δ*ccoA* mutants (SE8E/SE8H) versus the *ccoA* revertants (SE8R1, -2, -5, and 6) (Fig. 3A). This indel corresponded to an addition of a single cytosine residue in SE8R1A/B and SE8R2 (*copA11C* Δ*ccoA*Rev group 1), and a deletion of a single cytosine residue in SE8R5 and SE8R6 (*copA9C* Δ*ccoA*Rev group 2), in the same stretch of 10 consecutive cytosine residues between base pairs 231 to 241 of RCC01180 (called *copA* hereafter) (Fig. 3B). PCR amplification of this region from the genomic DNA from appropriate strains combined with sequencing validated these findings and established that in all Δ*ccoA* revertants, the *copA11C-copA9C* indel induced a frameshift mutation that inactivated the *copA* gene product (between amino acids at positions 78 to 81).

Δ*ccoA* Δ*copA* double mutants produce *cbb*$_3$-Cox and are Cu^s. A chromosomal deletion-insertion allele of *copA* (Δ*copA*) was constructed to demonstrate that its inactivation restored the production of *cbb*$_3$-Cox in a strain lacking *ccoA*. Introduction of this allele into the wild-type (MT1131) and Δ*ccoA* (SE8) strains yielded Δ*copA* (SE24) and Δ*copA* Δ*ccoA* (SE25) mutants, respectively. Like the Δ*ccoA* revertants (SE8Ri), the Δ*copA* Δ*ccoA* double mutant (SE25) produced wild-type-like *cbb*$_3$-Cox (determined by NADI staining [described under "Strains and culture conditions" in Materials and Methods]) on all media regardless of Cu^{2+} addition (Fig. 2A, right). It was also Cu^s to 50 μM $CuSO_4$, an amount that does not affect the growth of a wild-type strain or a Δ*ccoA* mutant (Fig. 3C, left). Moreover, introduction of a wild-type copy of *copA* carried by a transferable plasmid (pRK415_*CopA*) into a Δ*copA* Δ*ccoA* mutant (SE25) reversed its Cox$^+$ and Cu^s phenotypes back to those (Cox$^-$ and Cu^r) of the Δ*ccoA* mutant (SE8). Therefore, inactivation of CopA in the absence of CcoA restored the production of active *cbb*$_3$-Cox at the expense of forfeiting cellular Cu tolerance.

Δ*copA* single mutants are Cu^s but proficient for *cbb*$_3$-Cox production. An *R. capsulatus* Δ*copA* mutant (SE24) produced

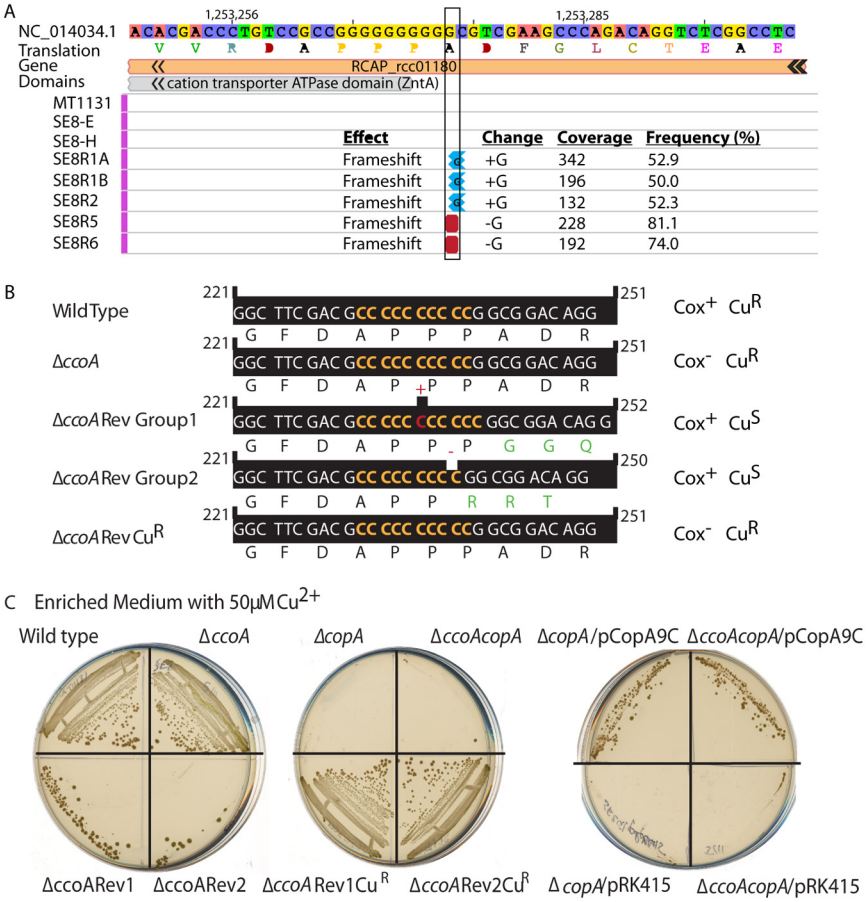

FIG 3 The Δ*ccoA* revertants contain a single cytosine indel mutation in the *copA* gene that inactivates CopA protein. (A) NGS results show the *R. capsulatus* genome region that contains the RCC01180 (*copA*) gene encoding CopA. The strains are listed to the left. MT1131 is the wild-type strain. SE8-E and SE8-H are two different isolates of SE8 (Δ*ccoA*). SE8R1A and SE8R1B are two different isolates of SE8R1 (Δ*ccoA*Rev1). SE8R2 (Δ*ccoA*Rev2), SE8R5 (Δ*ccoA*Rev5), and SE8R6 (Δ*ccoA*Rev6) strains are shown last. The whole genomes of the strains were sequenced and compared. The base pair changes and their effects and the related statistical data (coverage and frequency) are shown on the right. (B) The nucleotide sequence of *copA* between positions 221 and 251, together with the encoded amino acid sequence are shown for the wild type (MT1131), Δ*ccoA* (SE8E or -H), Δ*ccoA*Rev group 1 (SE8R1A or -B or SE8R2), Δ*ccoA*Rev group 2 (SE8R5 or SER6) and Δ*ccoA*Rev Cu^r (SE8R1Cu^R or SE8R2Cu^R) strains. The same sequence and reading frame are found in the wild-type, Δ*ccoA*, and Δ*ccoA*RevCu^R strains, which contain a wild-type *copA* allele with 10 consecutive cytosines. An insertion of one cytosine in Δ*ccoA*Rev group 1 (e.g., SE8R1) and a deletion of one cytosine in Δ*ccoA*Rev group 2 (e.g., SE8R5), resulting in 11 or 9 consecutive cytosines, respectively, and the frameshift mutations are also shown. (C) Cu^r and Cu^s phenotypes of wild-type (MT1131), Δ*ccoA* (SE8), Δ*copA* (SE24), Δ*ccoA* Δ*copA* (SE25), Δ*ccoA*Rev1 (SE8R1), Δ*ccoA*Rev2 (SE8R2), Δ*ccoA*Rev1Cu^R (SE8R1Cu^R), and Δ*ccoA*Rev2Cu^R (SE8R2Cu^R) strains were determined by their ability to grow on enriched MPYE medium supplemented with 50 μM $CuSO_4$. Under these conditions, Cu^s strains are unable to form colonies. Among the Cu^s strains, the Δ*ccoA*Rev1 (SE8R1) and Δ*ccoA*Rev2 (SE8R2) strains frequently yield Cu^r derivatives, whereas Δ*copA* (SE24) and Δ*ccoA* Δ*copA* (SE25) strains do not (compare the bottom of the left plate to the top of the middle plate). Similarly, the Δ*copA*/pCopA9C and Δ*copA* Δ*ccoA*/pCopA9C strains yield Cu^r derivatives, whereas the same strains with a plasmid lacking a *copA* allele (pRK415) do not yield any Cu^r derivatives (right plate).

wild-type-like cbb_3-Cox but was as Cu^s as the Δ*copA* Δ*ccoA* double mutant (SE25) or the Δ*ccoA* revertants (SE8Ri) (Fig. 3C). Thus, the Cu^s phenotype correlated with the absence of CopA. In agreement with this fact, complementation of a *ccoA* revertant (e.g., SE8R1) by a wild-type copy of *ccoA* (pSE3) also restored cbb_3-Cox production but not its Cu^s phenotype (data not shown).

If CopA is indeed involved in Cu detoxification, then the expression of *copA* should respond to the addition of Cu^{2+}, which was monitored by reverse transcription-PCR (RT-PCR). Total RNA was isolated from wild-type cells grown in enriched medium under respiratory conditions after incubation for 1 h with 1 μM $CuSO_4$. RNA samples were probed via RT-PCR using *copA*- and 16S rRNA (control)-specific primers. Semiquantitative image analyses indicated that incubation with Cu^{2+} induced *copA* expression (~3- to 4-fold), in agreement with its role in Cu detoxification, while 16S rRNA levels remained unchanged (Fig. 4). For further control, the expression of two other *R. capsulatus* P1B-type ATPases, RCC01042 with an unknown role (see below) and *ccoI* required for cbb_3-Cox production (12) were also analyzed in response to Cu^{2+} addition. While RCC01042 expression was unchanged, *ccoI* expression decreased (~2- to 3-fold) in response to Cu^{2+} addition.

Cu^r derivatives of Δ*ccoA* revertants switch back to wild-type *copA* and lose their ability to produce cbb_3-Cox. Upon exposure to exogenous Cu^{2+} (50 to 100 μM), spontaneous Cox$^+$ Δ*ccoA* revertants (SE8Ri) that carried the *copA11C-copA9C* indel mutations frequently yielded Cu-resistant (Cu^r) colonies that concomitantly lost their ability to produce cbb_3-Cox (Fig. 2B, right). DNA

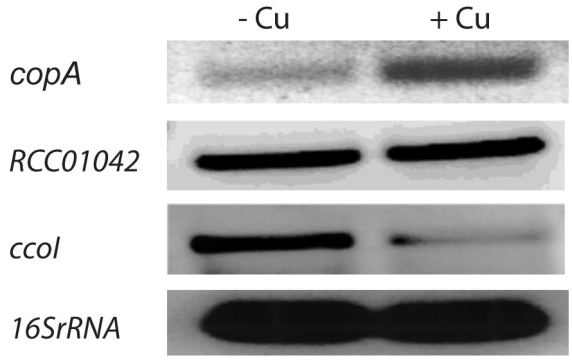

FIG 4 Transcriptional response of *copA*, *ccoI*, and RCC01042 genes to Cu^{2+} supplementation. RT-PCR data using total RNA extracted from a wild-type *R. capsulatus* strain (MT1131) grown under respiratory conditions in MPYE medium not supplemented with $CuSO_4$ (− Cu) or supplemented with 1 μM $CuSO_4$ (+ Cu) are shown. *copA* (RCC01180), RCC01042, and *ccoI* expression are shown together with the 16S rRNA expression, which is unaffected by the addition of Cu^{2+}. Note that *copA* expression is increased, whereas *ccoI* expression is decreased by Cu supplementation.

sequence analysis of two such derivatives (SE8R1Cu100 and SE8R2Cu100) revealed that in these strains, the mutant *copA11C* allele reverted back to the wild type by deletion of one cytosine residue at the same 10-cytosine repeat where the initial indel inactivating *copA* was located (Fig. 3B). Similarly, exposure to 50 μM Cu^{2+} of the Δ*copA* (SE24) and Δ*copA* Δ*ccoA* (SE25) strains harboring a plasmid with a mutant *copA9C* allele (pRK415_CopA9C) yielded Cu^r colonies (Fig. 3C, right). Sequencing of the plasmid-borne *copA* locus from these Cu^r colonies indicated that they switched back to a wild-type *copA* allele with the 10-cytosine repeat. Thus, the Δ*ccoA* suppressors (SE8Ri) could switch back and forth between the Cox^+ Cu^s and Cox^- Cu^r phenotypes depending on growth conditions, indicating that CcoA-CopA interplay controls both cbb_3-Cox production and Cu detoxification.

Other *R. capsulatus* paralogs of *copA* cannot substitute for its functions. Besides *copA* and *ccoI*, three other genes (RCC01042, RCC02064, and RCC02190) in the *R. capsulatus* genome are annotated as "copper or heavy metal translocating P-type ATPase." Their subgrouping based on ion selectivity determinants (20) suggested that RCC02190 and RCC02064 are not involved in Cu transport (see Table S4 in the supplemental material). RCC01042 could not be placed readily in any P1B subgroup, even though it is annotated as a "copper-translocating P-type ATPase *copA*." Its role was probed by constructing an insertion-deletion allele Δ*RCC01042*, which was introduced into the wild-type (MT1131) and Δ*ccoA* (SE8) strains to obtain SE26 and SE27, respectively. A mutant lacking RRC01042 (Δ*RCC01042* [SE26]) had no effect on Cu^s or Cox^+ phenotypes. Moreover, the Δ*ccoA* Δ*RCC02190* (SE31), Δ*ccoA* Δ*RCC01042* (SE27), and Δ*ccoA* Δ*ccoI* (SE13) double mutants were Cu^r and Cox^-, indicating that none of these P1B-type ATPases could functionally substitute for *copA* to suppress the cbb_3-Cox defect due to the absence of CcoA. We concluded that *R. capsulatus* contained only one CopA (i.e., RCC01180), which is involved in Cu detoxification, and also in cbb_3-Cox production when CcoA was absent.

DISCUSSION

Previously, we identified the MFS-type cytoplasmic membrane transporter CcoA as a component required for cbb_3-Cox production and showed that cellular Cu content decreased in its absence (16). Our findings indicated that CcoA is involved in Cu transport and trafficking into cbb_3-Cox. In this work, we obtained direct evidence by monitoring cellular ^{64}Cu uptake that the absence of CcoA affects Cu acquisition by *R. capsulatus* cells. We have also shown recently that *R. capsulatus* CcoA can complement the Cu import defect of a *Schizosaccharomyces pombe* Ctr-less mutant (17). Together, these data establish that CcoA is a cytoplasmic Cu importer. In a wild-type strain, ^{64}Cu uptake occurred more efficiently at a higher temperature (35°C versus 0°C), suggesting that CcoA-mediated Cu import may be energy dependent, which is consistent with the properties of MFS-type transporters (21).

The molecular basis of the Δ*ccoA* bypass suppressors was sought to gain insight into the link(s) between CcoA-mediated Cu import and cbb_3-Cox production. Initially, we used a genetic approach by constructing genomic libraries and transferring them into appropriate strains (Δ*ccoA* and Δ*ccoA*Rev), as done earlier (16). In this case, screening for transconjugants with expected Cox phenotypes to identify the suppressors was greatly hampered by the high frequency of spontaneous suppressors of Δ*ccoA*. To circumvent this difficulty, we used NGS technology-based whole-genome comparisons. In all cases examined, we found that Δ*ccoA* suppression was due to single-base-pair indel mutations located in a hot spot of consecutive 10 cytosines. The frameshift mutations located between amino acids at positions 78 to 81 of CopA inactivated this Cu exporter and rendered cells Cu^s. Interestingly, upon exposure to external Cu^{2+}, this same hot spot switched back to the wild type, reactivating CopA and rendering cells Cu^r but abolishing cbb_3-Cox production. Stretches of identical nucleotide repeats form mutational hot spots due to errors in DNA replication, referred to as "DNA polymerase slippage" (22–24), which frequently generates indels during the replication of repeats (25). In *R. capsulatus*, there are two repeats of 10 cytosines in *copA* and in hemolysin d (RCC03392), as well as one repeat of 12 cytosines in RCC03033 encoding a formate dehydrogenase subunit. It is currently unknown whether the occurrence of such repeats has any physiological role by forming hot spots for reversible activation/inactivation of genes via DNA polymerase slippage. Conceivably, the lack of cbb_3-Cox production due to the absence of CcoA could provide a selective advantage (e.g., in the natural habitat of *R. capsulatus*, *the* cbb_3-Cox activity is critical for anoxygenic photosynthesis) for inactivation of CopA at the expense of Cu^s. Similarly, elevated levels of external Cu could confer a selective advantage for reactivation of CopA to restore Cu tolerance when CcoA is inactive. Any link between the occurrence of these indels and the growth fitness due to cbb_3-Cox activity or the presence of Cu remains to be seen.

Suppression of the cbb_3-Cox deficiency induced by the absence of CcoA via the inactivation of the P1B-type ATPase *copA* at the expense of rendering cells Cu^s is novel. CopA homologues are integral membrane proteins that export Cu from the cytoplasm to the periplasm and play a major role against Cu toxicity (6). *R. capsulatus* CopA is 806 amino acids long, is predicted to form eight transmembrane helices, with an essential CPC motif in its sixth transmembrane helix and three (A, P, and N) domains common to all P-type ATPases. As observed in *Bradyrhizobium japonicum* (26) and *P. aeruginosa* (10), inactivation of *R. capsulatus copA* also rendered cells Cu^s without affecting cbb_3-Cox production. Thus, the Cu^s phenotype of the Δ*ccoA* suppressors originated from the inactivation of CopA, which establishes for the first time that

CopA is indirectly involved in cbb_3-Cox production when cells face cytoplasmic Cu shortage due to the absence of CcoA activity.

P1B-type ATPases are divided into five subgroups based on their ion selectivity determinants (20), with the *R. capsulatus* genome containing five such transporters (RCC01180, RCC01042, RCC01163, RCC02064, and RCC02190). CopA (RCC01180) has the MXXSS motif specific for the P1B-1-type subgroup for Cu^+/Ag^+, whereas CcoI (RCC01163) has the MSTS motif specific for the P1B-3-type subgroup for Cu^{2+}/Cu^+/Ag^+ in their eight transmembrane helices (see Table S4 in the supplemental material). Whether these structural differences between CopA and CcoI are the basis of their different efflux rates and whether the substrate redox states (20) are related to their physiological roles in Cu detoxification and cbb_3-Cox production is unknown. Of the remaining *R. capsulatus* P1B-type ATPases, RCC02190 belongs to the P1B-2 subgroup involved in transporting Zn^{2+}/Cd^{2+}/Pb^{2+}, and RCC02064 shows the characteristics of the P1B-4 subgroup that transports Co^{2+}. RCC01042 cannot be placed readily in any P1B subgroup. The data obtained in this work with RCC01042, and previously with RCC02190 (16), indicate that these transporters are not involved in Cu homeostasis or cbb_3-Cox production in *R. capsulatus.*

A major finding of this study is the functional interplay between CcoA and CopA that indirectly controls cbb_3-Cox production via cellular Cu homeostasis. Assuming that CcoA and CopA proteins are unlikely to interact physically, their interplay may be via a cytoplasmic Cu pool, which is replenished by CcoA and depleted by CopA (Fig. 5). Accordingly, a decrease in the size of this pool due to the absence of CcoA would render cells unable to produce cbb_3-Cox, whereas its increase due to the absence of CopA would restore cbb_3-Cox production while forfeiting a major Cu detoxification mechanism. These predictions are in agreement with our findings that homeostasis of the cytoplasmic Cu pool via the CcoA-CopA interplay is critical for growth fitness (i.e., cbb_3-Cox production) and survival (i.e., Cu toxicity) of bacterial cells (Fig. 5).

Earlier, the occurrence of a Cu pool in the *Saccharomyces cerevisiae* yeast and mouse mitochondrial matrix was described. Cu is liganded to a nonproteinaceous small molecule (CuL) (27) required for Cox biogenesis (28). The non-Cu-liganded form of this molecule (apoCuL) was also seen in the cytoplasm of these eukaryotic cells. These findings suggested that Cu-loaded CuL might be imported into the matrix via an inner membrane transporter in mitochondria (29). Somewhat similarly, a Cu chelator (CuL1) to neutralize Cu toxicity is excreted by some marine cyanobacteria (30). However, neither the chemical nature(s) of the mitochondrial or cyanobacterial CuL nor their roles in Cu acquisition are clear. So far, the methanobactins produced by methanotrophs are the only known small molecules involved in cellular Cu uptake (31). Recently, active-transport-dependent uptake of a Cu-methanobactin complex was shown in *Methylosinus trichosporium*, but how this process occurs is not yet known (31). MFS-type transporters are known to deliver iron-chelating siderophores (32, 33), which are reminiscent of methanobactins. Whether *R. capsulatus* produces a chalcophore is unknown, but the possibility that CcoA could import such a molecule into the cytoplasm is enticing. Finally, if a cytoplasmic Cu pool exists in *R. capsulatus* (Fig. 5), then how Cu is trafficked from this pool to CopA for detoxification and to CcoI for cbb_3-Cox production needs further studies.

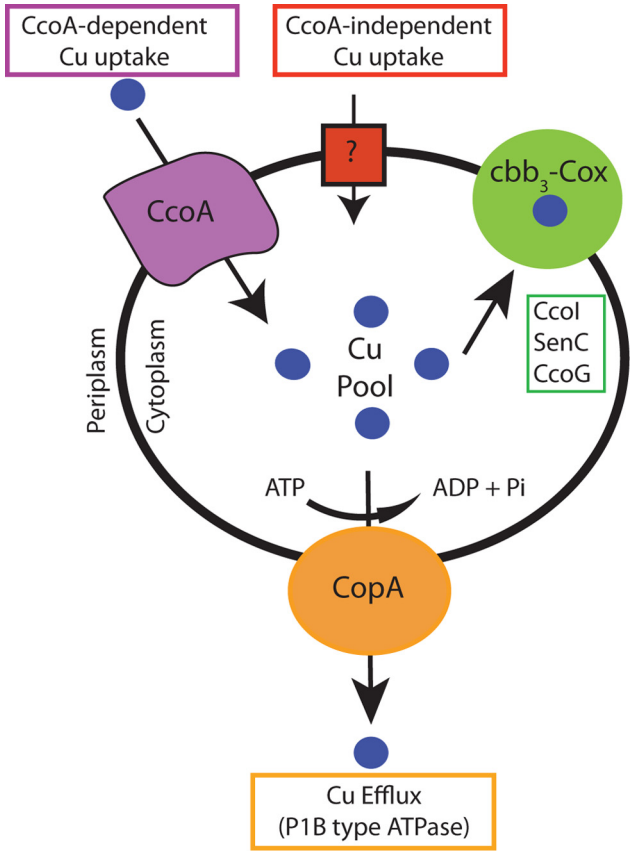

FIG 5 Model for Cu trafficking in *R. capsulatus*. The MFS-type transporter CcoA is required for high-affinity import into the cytoplasm of exogenous Cu, which is then delivered and inserted into cbb_3-Cox with the help of CcoI (the low-efflux P1B-type Cu ATPase), SenC, and CcoG. CopA (the high-efflux P1B-type Cu ATPase) extrudes Cu from the cytoplasm to the periplasm to avoid toxicity. A low-affinity Cu uptake system (indicated by ?) of unknown molecular nature is postulated to provide Cu to cbb_3-Cox in the absence of CcoA and in the presence of a high level (e.g., 5 μM) of exogenous Cu^{2+}. In a wild-type cell, the interplay between CcoA and CopA is proposed to occur via a cytoplasmic Cu pool to maintain cellular Cu homeostasis and efficient cbb_3-Cox production.

In bacteria, Cu efflux proteins are mostly well identified and characterized, but less is known about Cu importers (34, 35). It has been thought for a long time that cells would not import Cu because of its toxic nature. However, well-conserved high-affinity (i.e., Ctr1/3) and low-affinity (i.e., Fet4/Smf1) Cu transporters exist in eukaryotes (36, 37). The Ctr-type high-affinity transporters located in the plasma membrane are well studied, but no such transporter has been identified in bacteria. Furthermore, how Cu is imported into the mitochondria is also not known (29, 38). Indeed, our work demonstrates that CcoA is the first example of a bacterial MFS-type transporter that imports Cu (16). Whether similar Cu importers also exist in other bacteria and may be involved in the biogenesis of various Cox proteins and other cuproproteins is unknown. Currently, the only other known MFS-type Cu transporter is Mfc1 located in the forespore membranes of *Schizosaccharomyces pombe* yeast (39). Excitingly, recent heterologous expression of *R. capsulatus* CcoA in *S. pombe* lacking its own Ctr-type Cu importers showed that CcoA is functionally similar to these transporters in respect to their cytoplasmic Cu import ability (17).

In summary, this work provides the first identification of a homeostatic interplay between the Cu importer CcoA and the Cu exporter CopA that occurs in bacteria via a cytoplasmic Cu pool of vital importance for both Cu detoxification and biogenesis of major cuproproteins like Cox. Future studies addressing the chemical nature of this pool and the contributing partners trafficking Cu to cellular targets will be invaluable for our understanding of Cu homeostasis in bacteria.

MATERIALS AND METHODS

Strains and culture conditions. *R. capsulatus* strains (see Table S1 in the supplemental material) were grown on enriched medium (MPYE) (44), or Sistrom's minimal medium A, supplemented with appropriate antibiotics (spectinomycin [Spe], 10 μg ml^{-1}; kanamycin [Kan], 10 μg ml^{-1}; rifampin [Rif], 70 μg ml^{-1}; tetracycline [Tet], 2.5 μg ml^{-1}) at 35°C chemoheterotrophically (aerobic respiration) or photoheterotropically (anaerobic photosynthesis) in anaerobic jars with H_2- plus CO_2-generating gas packs (BBL Microbiology Systems, Cockeysville, MD) (40). As needed, the MPYE medium was supplemented with desired amounts of $CuSO_4$. *Escherichia coli* strains were grown on Luria-Bertani (LB) broth supplemented with appropriate antibiotics (ampicillin [Amp], 100 μg ml^{-1}; Spe, 50 μg ml^{-1}; Kan, 50 μg ml^{-1}; Tet, 12.5 μg ml^{-1}) as described earlier (40). Colonies producing an active Cox enzyme (Cox$^+$) were revealed via NADI staining prepared by mixing at a 1:1 (vol/vol) ratio 35 mM α-naphthol and 30 mM *N*,*N*,*N*′,*N*′-dimethyl-*p*-phenylene diamine (DMPD) dissolved in ethanol and water, respectively (41).

Molecular genetic techniques. Standard molecular genetic techniques were performed as described previously (42). The gene transfer agent (GTA) (43) of *R. capsulatus* was used to construct chromosomal knockout alleles of desired genes as described earlier (44). Genomic DNA was extracted from 10-ml cultures of the wild type (MT1131), Δ*ccoA* mutant (SE8), and its Cox$^+$ revertants (SE8Ri with i = 1 to 6) that were grown in MPYE medium by using the DNeasy Blood & Tissue kit (Qiagen Inc.). The quality and quantity of the isolated genomic DNA were analyzed by using a Nanodrop spectrophotometer and by agarose gel electrophoresis prior to library preparations for NGS.

To construct a deletion-insertion allele of *copA* (*R. capsulatus* RCC01180, initially annotated as *copA*), a DNA fragment encompassing ~500 bp 5′ upstream and 3′ downstream of *copA*, including its promoter region, was PCR amplified using wild-type (MT1131) chromosomal DNA as a template, and the primers CopAFwd (Fwd stands for forward) and CopARev (Rev stands for reverse) containing 5′ SacI and 3′ KpnI sites, respectively (see Table S2 in the supplemental material). This DNA fragment was digested with appropriate restriction enzymes and cloned into the respective sites of pBluescript II-KS+ and pRK415 to yield the plasmids pBS_CopA and pRK415_CopA, respectively (Table S1). Starting with pBS_CopA, ~1,100 bp of *copA* was deleted by using the primers CopAdelfwd2 (del stands for deletion) and CopAdelrev2 (Table S2), which amplified the remaining flanking regions of *copA* and the vector. A Kan^r cassette from plasmid pKD4 (45) was ligated between the two flanking regions of *copA* to yield pBS_Δ*copA* carrying the Δ(*copA*::*kan*) allele. The SacI-KpnI fragment of pBS_Δ*copA* was cloned into the respective sites of plasmid pRK415 to yield pRK415_Δ*copA*. The latter plasmid was used to obtain the Δ*copA* knockout mutants SE24 and SE25 by GTA crosses with the wild type (MT1131) and a Δ*ccoA* (SE8) mutant, respectively, as the recipients (Table S1).

To construct a deletion-insertion allele of *R. capsulatus copA* paralog RCC01042 (initially also annotated as *copA*), a DNA fragment encompassing this open reading frame, including its promoter region, was PCR amplified using the primers RCC01042Fwd and RCC01042Rev (see Table S2 in the supplemental material) and cloned into the SacI and KpnI sites of pBluescript II-KS+ and pRK415 as described above, yielding plasmids pBS_CopA1 and pRK415_CopA1. Starting with pBS_CopA1, a knockout allele Δ(*RCC01042*::*gen*) was constructed as described above, by deleting the ~1100 bp of RCC01042 using primers RCC01042delF and RCC01042delR (Table S2) and ligating a gentamicin resistance cassette, which was PCR amplified from *R. capsulatus* B10S-T7 strain (46), between the two flanking regions of RCC01042 to obtain pBS_ΔRCC01042. The SacI-KpnI DNA fragment of pBS_ΔRCC01042 was cloned into pRK415 to yield pRK415_RCC01042, which was used to construct the SE26 and SE27 mutants by GTA crosses with the wild-type (MT1131) and Δ*ccoA* (SE8) strains, respectively, as the recipients (Table S1).

RT-PCR analyses. For reverse transcription-PCR (RT-PCR) analyses, appropriate *R. capsulatus* strains were grown in MPYE medium to mid-log phase (optical density at 685 nm [OD_{685}] of 0.8 to 1.0). An amount of culture corresponding to ~10^9 cells was centrifuged, and the cells were incubated in TE buffer (10 mM Tris-HCl, 0.5 mM EDTA [pH 7.0]) containing 10 mg/ml lysozyme for 15 min at 37°C and passed five times through a 0.8-mm needle into RNase-free tubes. Total RNA was isolated using the GE Healthcare Mini Spin kit, according to the manufacturer's instructions. Two to five micrograms of total RNA was treated with DNase I for 30 min at 25°C in the presence of RNase inhibitor RNasin. Fifty to 200 ng of DNA and RNase-free RNA was used for RT-PCR reaction with the OneStep RT-PCR Qiagen kit. A 25-μl total reaction mixture volume consisted of 5 μl reaction buffer, 1 μl deoxynucleoside triphosphate (dNTP), 0.1 nmol of each appropriate primer (see Table S2 in the supplemental material), and 1 μl of enzyme mix (reverse transcriptase and DNA polymerase) and water up to 25 μl. Similar PCR reactions with the same primers and RNA amounts were performed as controls for the absence of genomic DNA contamination by using the PHUSION PCR kit (NEB Inc., MA), and samples were analyzed using a 1.2% agarose gel.

Cu^{2+} sensitivity assays. Strains to be tested for their Cu sensitivity were grown to exponential phase (OD_{630} of ~0.5) in enriched MPYE medium under respiratory growth conditions. Approximately 2×10^7 cells were mixed with 4 ml MPYE medium containing 0.7% top agar and poured on top of 10-ml MPYE plates. After solidification of agar, Whatman 3MM paper disks (3-mm diameter) soaked with 8 μl of the desired concentrations of $CuSO_4$ solutions were placed on agar surfaces. The plates were incubated for 2 days at 35°C under respiratory growth conditions and scanned. $CuSO_4$ toxicity responses of the strains were determined by measuring the size of growth incubation zones around the Cu^{2+}-containing paper disks (16).

Radioactive ^{64}Cu uptake assay. Cu uptake by whole cells was measured using radioactive ^{64}Cu obtained from Mallinckrodt Institute of Radiology, Washington University Medical School (effective specific activity [ESA] of ~1.84×10^4 mCi/μmol at noon of the shipping day; half-life, ~12 h). Appropriate strains were grown overnight in 15 ml MPYE medium and harvested at mid-exponential or late exponential phase (OD_{630} of ~0.6 to 0.8), centrifuged, washed once with 5 ml fresh MPYE medium, and resuspended in ~1 ml. The total numbers of cells were determined spectrophotometrically (1 OD_{630} unit = 7.5×10^8 cells/ml), and all cultures were normalized to the same number of cells per milliliter of MPYE medium. The ^{64}Cu uptake assay mixture contained ~7×10^8 cells (added as ~100 to 200 μl of MPYE medium), a volume of ^{64}Cu corresponding to a total of ~10^7 cpm, and completed to a total volume of 500 μl with citrate buffer (50 mM sodium citrate, 5% glucose [pH 6.5]). One set was incubated at 0°C in an ice bath, and another set was incubated at 35°C in a water bath. The uptake reaction was started by the addition of a volume of $^{64}CuCl_2$ corresponding to ~10^7 cpm determined immediately before use. At each time point (0, 1, 2, 5, 10, 20, and 30 min), 50-μl aliquots were transferred to ice-cold Eppendorf tubes containing 50 μl of 1 mM $CuCl_2$ and 50 μl of 50 mM EDTA (pH 6.5) to terminate the uptake reaction. Samples were kept on ice until the end of the assay and centrifuged for 3 min at 10,000 rpm, supernatants were discarded, and pellets were washed twice with 100 μl of ice-cold 50 mM EDTA solution, resuspended in 1 ml scintillation liquid, and counted by using a scintillation counter with a wide open window.

Next-generation genome sequencing and analysis. The NGS of the genomes of eight *R. capsulatus* strains, the wild type (MT1131), two independent isolates of a Δ*ccoA* mutant (SE8H and SE8E), and four Δ*ccoA*

revertant (two independent isolates of SE8R1 [SE8R1A and SE8R1B], SE8R2, SE8R5, SE8R6) mutants (see Table S1 in the supplemental material) was performed by Covance Genomics Laboratory LLC, Seattle, WA. The use of multiple replicates of the same strains in our experimental design allowed ready accounting of both experimental artifacts and biological variability that otherwise could significantly affect final analyses. Genomic DNA was sheared by using a Covaris Adaptive Focused Acoustics system (Covaris, Woburn, MA), and genomic DNA libraries with insert size between 200 and 300 bp were prepared by using Illumina TrueSeq DNA sample prep kit for paired-end sequencing, according to the manufacturer's instructions (Illumina Inc.). The resulting genomic DNA libraries were sequenced by using an Illumina HiSeq2000 sequencing machine to yield 12 to 15 million reads of 100-bp lengths. All reads were aligned to the *R. capsulatus* SB1003 reference genome (GenBank accession no. CP001312.1 and CP001313.1) by using the bow tie alignment algorithm (47), and SNP and indels were identified by using SAMtools (48). Illumina standard quality check and filtering conditions were used. Sequence reads obtained with the laboratory wild-type strain MT1131 were aligned against the *R. capsulatus* SB1003 reference genome, and the SNPs and indels that it contained were defined (Table S3). Then, the sequence reads obtained with the Δ*ccoA* mutants (SE8E and SE8H) and revertants (SE8R1A, SE8R1B, SE8R2, SE8R5, and SE8R6) were aligned against the reference genome, and they were also compared with MT1131 sequence reads to define the SNPs and indels that all strains contained using Integrative Genomics Viewer (IGV) software (49). All NGS analyses, whole-genome comparisons, and defined SNP and indel data are available at http://networks.systemsbiology.net/rcaps/.

SUPPLEMENTAL MATERIAL

Supplemental material for this article may be found at http://mbio.asm.org/lookup/suppl/doi:10.1128/mBio.01055-13/-/DCSupplemental.

Table S1, DOCX file, 0.1 MB.
Table S2, DOCX file, 0.1 MB.
Table S3, DOCX file, 0.1 MB.
Table S4, DOCX file, 0.1 MB.

ACKNOWLEDGMENTS

This work was supported by the Division of Chemical Sciences, Geosciences and Biosciences, Office of Basic Energy Sciences of the U.S. Department of Energy through grant DE-FG02-91ER20052 and NIH GM 38237 to F.D. and the Deutsche Forschungsgemeinschaft (DFG-GRK1478 to H.G.K. and DFG-FOR 929 to H.G.K.) and from the German-French-University (DFH) PhD College on "Membranes and Membrane Proteins" grants to H.G.K.

REFERENCES

1. **Banci L, Bertini I, McGreevy KS, Rosato A.** 2010. Molecular recognition in copper trafficking. Nat. Prod. Rep. **27:**695–710. http://dx.doi.org/10.1039/b906678k.
2. **Samanovic MI, Ding C, Thiele DJ, Darwin KH.** 2012. Copper in microbial pathogenesis: meddling with the metal. Cell Host Microbe **11:**106–115. http://dx.doi.org/10.1016/j.chom.2012.01.009.
3. **Macomber L, Imlay JA.** 2009. The iron-sulfur clusters of dehydratases are primary intracellular targets of copper toxicity. Proc. Natl. Acad. Sci. U. S. A. **106:**8344–8349. http://dx.doi.org/10.1073/pnas.0812808106.
4. **Rae TD, Schmidt PJ, Pufahl RA, Culotta VC, O'Halloran TV.** 1999. Undetectable intracellular free copper: the requirement of a copper chaperone for superoxide dismutase. Science **284:**805–808. http://dx.doi.org/10.1126/science.284.5415.805.
5. **Luk E, Jensen LT, Culotta VC.** 2003. The many highways for intracellular trafficking of metals. J. Biol. Inorg. Chem. **8:**803–809. http://dx.doi.org/10.1007/s00775-003-0482-3.
6. **Argüello JM, Eren E, González-Guerrero M.** 2007. The structure and function of heavy metal transport P1B-ATPases. Biometals **20:**233–248. http://dx.doi.org/10.1007/s10534-006-9055-6.
7. **de Bie P, Muller P, Wijmenga C, Klomp LW.** 2007. Molecular pathogenesis of Wilson and Menkes disease: correlation of mutations with molecular defects and disease phenotypes. J. Med. Genet. **44:**673–688. http://dx.doi.org/10.1136/jmg.2007.052746.
8. **Zheng Z, White C, Lee J, Peterson TS, Bush AI, Sun GY, Weisman GA, Petris MJ.** 2010. Altered microglial copper homeostasis in a mouse model of Alzheimer's disease. J. Neurochem. **114:**1630–1638. http://dx.doi.org/10.1111/j.1471-4159.2010.06888.x.
9. **Leonhardt K, Gebhardt R, Mössner J, Lutsenko S, Huster D.** 2009. Functional interactions of Cu-ATPase ATP7B with cisplatin and the role of ATP7B in the resistance of cells to the drug. J. Biol. Chem. **284:**7793–7802. http://dx.doi.org/10.1074/jbc.M805145200.
10. **González-Guerrero M, Raimunda D, Cheng X, Argüello JM.** 2010. Distinct functional roles of homologous Cu^+ efflux ATPases in *Pseudomonas aeruginosa*. Mol. Microbiol. **78:**1246–1258. http://dx.doi.org/10.1111/j.1365-2958.2010.07402.x.
11. **Raimunda D, González-Guerrero M, Leeber BW, III, Argüello JM.** 2011. The transport mechanism of bacterial Cu^+-ATPases: distinct efflux rates adapted to different function. Biometals **24:**467–475. http://dx.doi.org/10.1007/s10534-010-9404-3.
12. **Koch HG, Winterstein C, Saribas AS, Alben JO, Daldal F.** 2000. Roles of the *ccoGHIS* gene products in the biogenesis of the cbb_3-type cytochrome *c* oxidase. J. Mol. Biol. **297:**49–65. http://dx.doi.org/10.1006/jmbi.2000.3555.
13. **Pereira MM, Sousa FL, Veríssimo AF, Teixeira M.** 2008. Looking for the minimum common denominator in haem-copper oxygen reductases: towards a unified catalytic mechanism. Biochim. Biophys. Acta **1777:**929–934. http://dx.doi.org/10.1016/j.bbabio.2008.05.441.
14. **Cobine PA, Pierrel F, Winge DR.** 2006. Copper trafficking to the mitochondrion and assembly of copper metalloenzymes. Biochim. Biophys. Acta **1763:**759–772. http://dx.doi.org/10.1016/j.bbamcr.2006.03.002.
15. **Gray KA, Grooms M, Myllykallio H, Moomaw C, Slaughter C, Daldal F.** 1994. *Rhodobacter capsulatus* contains a novel *cb*-type cytochrome *c* oxidase without a Cu_A center. Biochemistry **33:**3120–3127. http://dx.doi.org/10.1021/bi00176a047.
16. **Ekici S, Yang H, Koch HG, Daldal F.** 2012. Novel transporter required for biogenesis of cbb_3-type cytochrome *c* oxidase in *Rhodobacter capsulatus*. mBio **3**(1):293–311. http://dx.doi.org/10.1128/mBio.00293-11.
17. **Beaudoin J, Ekici S, Daldal F, Ait-Mohand S, Guérin B, Labbé S.** 2013. Copper transport and regulation in *Schizosaccharomyces pombe*. Biochem. Soc. Trans. **41:**1679–1686. http://dx.doi.org/10.1042/BST2013089.
18. **Zannoni D, Prince RC, Dutton PL, Marrs BL.** 1980. Isolation and characterization of a cytochrome c_2-deficient mutant of *Rhodopseudomonas capsulata*. FEBS Lett. **113:**289–293. http://dx.doi.org/10.1016/0014-5793(80)80611-9.
19. **Strnad H, Lapidus A, Paces J, Ulbrich P, Vlcek C, Paces V, Haselkorn R.** 2010. Complete genome sequence of the photosynthetic purple nonsulfur bacterium *Rhodobacter capsulatus* SB 1003. J. Bacteriol. **192:**3545–3546. http://dx.doi.org/10.1128/JB.00366-10.
20. **Argüello JM.** 2003. Identification of ion-selectivity determinants in heavy-metal transport P1B-type ATPases. J. Membr. Biol. **195:**93–108. http://dx.doi.org/10.1007/s00232-003-2048-2.
21. **Reddy VS, Shlykov MA, Castillo R, Sun EI, Saier MH, Jr.** 2012. The major facilitator superfamily (MFS) revisited. FEBS J. **279:**2022–2035. http://dx.doi.org/10.1111/j.1742-4658.2012.08588.x.
22. **Baumann B, Potash MJ, Köhler G.** 1985. Consequences of frameshift mutations at the immunoglobulin heavy chain locus of the mouse. EMBO J. **4:**351–359.
23. **Strauss BS.** 1999. Frameshift mutation, microsatellites and mismatch repair. Mutat. Res. **437:**195–203. http://dx.doi.org/10.1016/S1383-5742(99)00066-6.
24. **Streisinger G, Owen J.** 1985. Mechanisms of spontaneous and induced frameshift mutation in bacteriophage T4. Genetics **109:**633–659.
25. **Dieringer D, Schlötterer C.** 2003. Two distinct modes of microsatellite mutation processes: evidence from the complete genomic sequences of nine species. Genome Res. **13:**2242–2251. http://dx.doi.org/10.1101/gr.1416703.
26. **Preisig O, Zufferey R, Hennecke H.** 1996. The *Bradyrhizobium japonicum fixGHIS* genes are required for the formation of the high-affinity cbb_3-type cytochrome oxidase. Arch. Microbiol. **165:**297–305. http://dx.doi.org/10.1007/s002030050330.
27. **Cobine PA, Ojeda LD, Rigby KM, Winge DR.** 2004. Yeast contain a non-proteinaceous pool of copper in the mitochondrial matrix. J. Biol. Chem. **279:**14447–14455. http://dx.doi.org/10.1074/jbc.M312693200.
28. **Cobine PA, Pierrel F, Bestwick ML, Winge DR.** 2006. Mitochondrial

matrix copper complex used in metallation of cytochrome oxidase and superoxide dismutase. J. Biol. Chem. **281:**36552–36559. http://dx.doi.org/10.1074/jbc.M606839200.
29. **Vest KE, Leary SC, Winge DR, Cobine PA.** 2013. Copper import into the mitochondrial matrix in *Saccharomyces cerevisiae* is mediated by Pic2, a mitochondrial carrier family protein. J. Biol. Chem. **288:**23884–23892. http://dx.doi.org/10.1074/jbc.M113.470674.
30. **Moffett JW, Brand LE.** 1996. Production of strong, extracellular Cu chelators by marine cyanobacteria in response to Cu stress. Limnol. Oceanogr. **41:**388–395. http://dx.doi.org/10.4319/lo.1996.41.3.0388.
31. **Balasubramanian R, Kenney GE, Rosenzweig AC.** 2011. Dual pathways for copper uptake by methanotrophic bacteria. J. Biol. Chem. **286:**37313–37319. http://dx.doi.org/10.1074/jbc.M111.284984.
32. **Franza T, Mahé B, Expert D.** 2005. *Erwinia chrysanthemi* requires a second iron transport route dependent of the siderophore achromobactin for extracellular growth and plant infection. Mol. Microbiol. **55:**261–275.
33. **Furrer JL, Sanders DN, Hook-Barnard IG, McIntosh MA.** 2002. Export of the siderophore enterobactin in *Escherichia coli*: involvement of a 43 kDa membrane exporter. Mol. Microbiol. **44:**1225–1234. http://dx.doi.org/10.1046/j.1365-2958.2002.02885.x.
34. **Hood MI, Skaar EP.** 2012. Nutritional immunity: transition metals at the pathogen-host interface. Nat. Rev. Microbiol. **10:**525–537. http://dx.doi.org/10.1038/nrmicro2836.
35. **Kim BE, Nevitt T, Thiele DJ.** 2008. Mechanisms for copper acquisition, distribution and regulation. Nat. Chem. Biol. **4:**176–185. http://dx.doi.org/10.1038/nchembio.72.
36. **Dancis A, Haile D, Yuan DS, Klausner RD.** 1994. The *Saccharomyces cerevisiae* copper transport protein (Ctr1p). Biochemical characterization, regulation by copper, and physiologic role in copper uptake. J. Biol. Chem. **269:**25660–25667.
37. **Liu XF, Culotta VC.** 1999. Mutational analysis of *Saccharomyces cerevisiae* Smf1p, a member of the Nramp family of metal transporters. J. Mol. Biol. **289:**885–891. http://dx.doi.org/10.1006/jmbi.1999.2815.
38. **Festa RA, Thiele DJ.** 2011. Copper: an essential metal in biology. Curr. Biol. **21:**877–883. http://dx.doi.org/10.1016/j.cub.2011.09.040.
39. **Beaudoin J, Ioannoni R, López-Maury L, Bähler J, Ait-Mohand S, Guérin B, Dodani SC, Chang CJ, Labbé S.** 2011. Mfc1 is a novel forespore membrane copper transporter in meiotic and sporulating cells. J. Biol. Chem. **286:**34356–34372. http://dx.doi.org/10.1074/jbc.M111.280396.
40. **Jenney FE, Jr, Daldal F.** 1993. A novel membrane-associated *c*-type cytochrome, cyt c_y, can mediate the photosynthetic growth of *Rhodobacter capsulatus* and *Rhodobacter sphaeroides*. EMBO J. **12:**1283–1292.
41. **Marrs B, Gest H.** 1973. Genetic mutations affecting the respiratory electron-transport system of the photosynthetic bacterium *Rhodopseudomonas capsulata*. J. Bacteriol. **114:**1045–1051.
42. **Sambrook J, Russell DW.** 2001. Molecular cloning: a laboratory manual, 3rd ed. Cold Spring Harbor Laboratory Press, Cold Spring Harbor, NY.
43. **Yen HC, Hu NT, Marrs BL.** 1979. Characterization of the gene transfer agent made by an overproducer mutant of *Rhodopseudomonas capsulata*. J. Mol. Biol. **131:**157–168. http://dx.doi.org/10.1016/0022-2836(79)90071-8.
44. **Daldal F, Cheng S, Applebaum J, Davidson E, Prince RC.** 1986. Cytochrome c_2 is not essential for photosynthetic growth of *Rhodopseudomonas capsulata*. Proc. Natl. Acad. Sci. U. S. A. **83:**2012–2016. http://dx.doi.org/10.1073/pnas.83.7.2012.
45. **Myllykallio H, Zannoni D, Daldal F.** 1999. The membrane-attached electron carrier cytochrome c_y from *Rhodobacter sphaeroides* is functional in respiratory but not in photosynthetic electron transfer. Proc. Natl. Acad. Sci. U. S. A. **96:**4348–4353. http://dx.doi.org/10.1073/pnas.96.8.4348.
46. **Katzke N, Arvani S, Bergmann R, Circolone F, Markert A, Svensson V, Jaeger KE, Heck A, Drepper T.** 2010. A novel T7 RNA polymerase dependent expression system for high-level protein production in the phototrophic bacterium *Rhodobacter capsulatus*. Protein Expr. Purif. **69:**137–146. http://dx.doi.org/10.1016/j.pep.2009.08.008.
47. **Langmead B, Trapnell C, Pop M, Salzberg SL.** 2009. Ultrafast and memory-efficient alignment of short DNA sequences to the human genome. Genome Biol. **10:**R25. http://dx.doi.org/10.1186/gb-2009-10-3-r25.
48. **Li H, Handsaker B, Wysoker A, Fennell T, Ruan J, Homer N, Marth G, Abecasis G, Durbin R, 1000 Genome Project Data Processing Subgroup.** 2009. The Sequence Alignment/map format and SAMtools. Bioinformatics **25:**2078–2079. http://dx.doi.org/10.1093/bioinformatics/btp352.
49. **Robinson JT, Thorvaldsdóttir H, Winckler W, Guttman M, Lander ES, Getz G, Mesirov JP.** 2011. Integrative genomics viewer. Nat. Biotechnol. **29:**24–26. http://dx.doi.org/10.1038/nbt.1754.